



Research Article

# Tungsten oxide modified AITUD-1 mesoporous acid catalyst for synthesis of thiazole aryl imines and phenylhydrazones

M. Rajarajan<sup>1</sup> · M. P. Pachamuthu<sup>2</sup>  · G. Thirunarayanan<sup>3</sup> · G. Vanangamudi<sup>4</sup> · Mohamed S. Hamdy<sup>5</sup>

© Springer Nature Switzerland AG 2019

## Abstract

A non-surfactant route synthesized mesoporous AITUD-1 (Si/Al = 25) with interconnected porous networks effectively utilized as a support for 10 wt% tungsten oxide (WO<sub>3</sub>) dispersions. The synthesized WO<sub>3</sub>/AITUD-1 catalyst was characterized by different techniques. N<sub>2</sub> sorption and XRD studies were confirmed its amorphous mesoporous nature, which measured a pore diameter of 6.4 nm and a surface area of 510 m<sup>2</sup> g<sup>-1</sup>. Presence of WO<sub>3</sub> on the pores and silica TUD-1 wormhole structure were evaluated by techniques including DRUV Visible and FT-Raman. The catalyst possessed both Lewis (L) and Brønsted (B) acidity, as measured by pyridine adsorbed FT-IR, which is responsible for the catalyst activity. WO<sub>3</sub>/AITUD-1 acid catalyst showed an excellent catalytic performance yield of about 80% at 80 °C in reflux condition, for different 1-substituted benzylidene 4-methylbenzo[*d*]thiazole-2-amines (thiazole based aryl imines) and substituted phenylhydrazone compounds.

**Electronic supplementary material** The online version of this article (<https://doi.org/10.1007/s42452-019-0928-z>) contains supplementary material, which is available to authorized users.

✉ M. P. Pachamuthu, pachachem@gmail.com; pachamuthu@bitsathy.ac.in | <sup>1</sup>Department of Chemistry, Thiruvalluvar Arts and Science College, Kurinjipadi, Tamil Nadu 607302, India. <sup>2</sup>Department of Chemistry, Bannari Amman Institute of Technology, Sathyamangalam, Erode 638401, India. <sup>3</sup>Department of Chemistry, Annamalai University, Annamalainagar 608002, India. <sup>4</sup>PG & Research Department of Chemistry, Government Arts College, C-Mutlur, Chidambaram, 608102, India. <sup>5</sup>Chemistry Department, College of Science, King Khalid University, P.O. Box 9004, Abha 61413, Saudi Arabia.

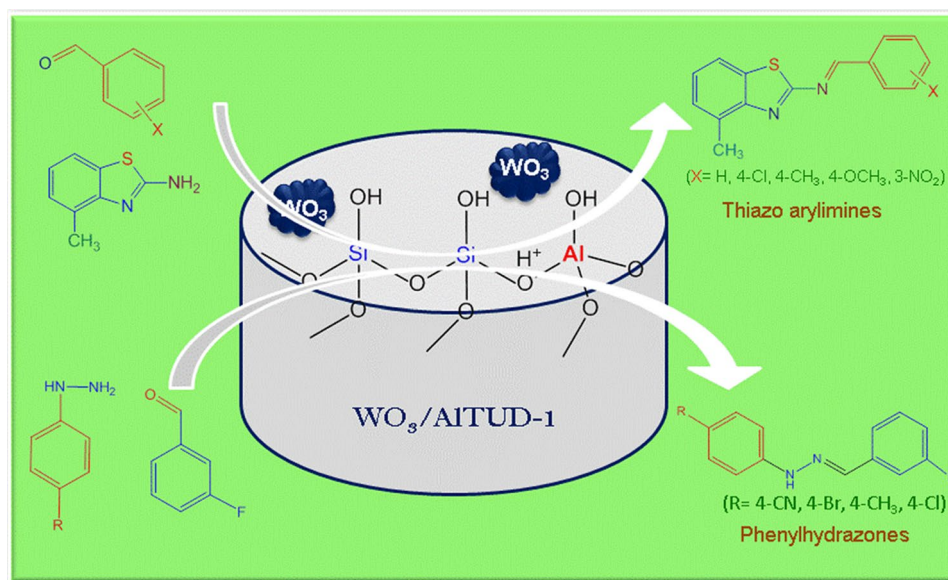


SN Applied Sciences (2019) 1:940 | <https://doi.org/10.1007/s42452-019-0928-z>

Received: 19 June 2019 / Accepted: 15 July 2019 / Published online: 30 July 2019

SN Applied Sciences  
A SPRINGER NATURE journal

## Graphic abstract



**Keywords** Mesoporous · Catalyst · Solid acid · AITUD-1 · Schiff bases

## 1 Introduction

Hydrazones and Schiff bases are versatile class of organic compounds. It contains azomethines ( $R-CH=NR'$ ) functionality, which is the common feature for both hydrazone and Schiff bases. These azomethine derivatives are interesting compounds because of their remarkable array of biological activity [1, 2]. The literature reviews have shown that Schiff's base possess a broad range of physiological activities such as anti-microbial, antidiabetic, anthelmintic, anti-tuberculosis, anti-inflammatory, anti-convulsant, antitumor, antioxidant, anti-viral, antihypertensive and anti-diabetic activities [3]. Vicini et al. [4] have synthesized Benzo[d]isothiazole derivatives by the reaction of benzo[d]isothiazol-3-ylamine with substituted benzaldehydes in anhydrous benzene and the synthesized compounds were studied for biological evaluation. Meanwhile, owing to the unique  $R, R'-C=N-N-R''-R'''$  structure (hydrazone) show a variety of antimicrobial activities, such as herbicide [5], anticonvulsant [6], antimicrobial [7], mitocidal [8], antioxidant [9], and anticancer activities [10]. Recently, Rajarajan et al. [11] have synthesized phenylhydrazone derivatives and studied its antimicrobial activities.

Many green acid catalysts like  $BiCl_3$ -K10 [12],  $MgSO_4$ -PPTL [13],  $SiO_2$ - $NaHSO_4$  [14], PSSA [15], K-10 montmorillonite [16], Tandam catalyst [17],  $MgSO_4$ -PPTS [18],  $Ti(OR)_4$  [19] and  $P_2O_5$ - $SiO_2$  [20] have been utilized for Schiff base and hydrazone compounds synthesis. However, there is a noticeable development required in catalyst structures. Typically, in the heterogeneous catalysts based organic transformation

reactions, catalysts are revealing its good acidity, high surface area, stable and recyclability. Besides, various metal ions ( $M^{x+}$ ) and metal oxides ( $M_xO_y$ ) modified mesoporous materials (MCM-41, SBA-15, KIT-6, and TUD-1) have also been employed as a solid acid catalyst for many industrial important organic conversions. Notably, isolated tungsten (W) or oxides of tungsten-based mesoporous catalyst have received much attention, due to its acidity and redox properties [21–24]. Kundu et al. [25] reported that the effective utilization of tungstic acid modified SBA-15 acid catalyst for one-pot condensation reaction of three components. Recently, W-TUD-1 [26] and  $WO_4$ /TiTUD-1 [27] type mesoporous catalysts were tested as a solid acid catalyst for industrially relevant Prins cyclisation and esterification reactions. Hence, we have taken efforts for the synthesis of new  $WO_3$  modified AITUD-1 catalyst and examined its activity for thiazole based aryl imines (1-substituted benzylidene 4-methylbenzo[d]thiazole-2-amines) and substituted phenylhydrazone compounds preparation. These synthesized catalyst and products are characterized by different spectral techniques.

## 2 Experimental

### 2.1 Catalyst synthesis

AITUD-1 with Si/Al molar ratio of 25 was synthesized by sol-gel, hydrothermal method based on our previously reported procedure [28]. In a typical catalyst preparation,

21 g of tetraethyl orthosilicate (TEOS, Sigma Aldrich) and aluminium isopropoxide (Al (isop)<sub>3</sub>, Sigma Aldrich) were stirred for 10 min. A mixture of 14 g of triethanolamine (TEA, SRL) and 5 g of water was then added to the above mixture and stirred vigorously for 1 h. Finally, 19.8 g of tetraethylammonium hydroxide (TEAOH, 35%, Sigma Aldrich) was slowly added to the prior solution under continuous stirring for another 2 h. The above-obtained gel was aged at 30 °C for 24 h and then dried at 100 °C for 24 h. The final solid was kept for hydrothermal treatment at (180 °C) for 8 h and successively calcined at 600 °C for 10 h to eliminate the organic molecules and water. 10 wt% of tungsten oxide supported on the amorphous AITUD-1 catalyst (preheated 250 °C for 2 h) is prepared by the conventional impregnation method using tungstic acid (Aldrich) solution. The mixture was stirred for 12 h and then dried at 100 °C for 6 h. Finally, the sample was calcined at 550 °C for 6 h in an air atmosphere. The obtained material was mentioned as WO<sub>3</sub>/AITUD-1.

## 2.2 Catalyst characterizations

Powder XRD patterns were obtained high angle region employed Rigaku diffractometer using Cu K $\alpha$  ray ( $\lambda = 1.5418 \text{ \AA}$ ). FT-IR spectrum is measured on a Bruker spectrometer (Tensor) in DRIFT resolution of 4 cm<sup>-1</sup>. BET the specific surface area and BJH pore size distribution were determined from nitrogen sorption using Quantachrome (*QuadrasorbSI*) porosimeter equipment (77 K) at liquid nitrogen temperature. The morphology was examined by scanning electron micrographs (SEM) imaging using ESEM Quanta 200 with a resolution of 10 kV. Transmission electron microscopy (TEM) was performed on a FEI Tecnai G2 fitted with a CCD camera. Diffuse reflectance ultraviolet–visible (DR UV–Vis) spectrum of the sample was recorded on a Thermoscientific spectrometer (Evolution 600) with a diffuse reflectance attachment, using BaSO<sub>4</sub> as the reference. FT-Raman spectra of the samples were attained on a Bruker system 1000R using 1064 nm (Nd:YAG laser source) excitation source.

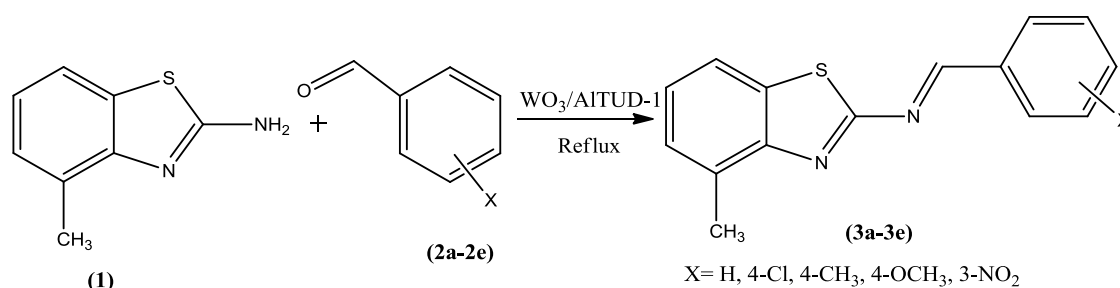
## 2.3 Synthesis of 1-substituted benzylidene-4-methylbenzo[d]thiazole-2-amine over WO<sub>3</sub>/AITUD-1

In a typical reaction, equimolar quantities of substituted benzaldehyde (0.01 mol), 4-methylbenzo[d]thiazol-2-amine (0.01 mol) and 20 mL of absolute ethanol with 0.1 g of WO<sub>3</sub>/AITUD-1 catalyst were added to 50 mL round bottom (RB) flask fitted with temperature controlled oil bath and magnetic stirrer (Scheme 1). This solution was refluxed for 4 h and the reaction progress is monitored by TLC. After completion, the reaction mixture was cooled and washed with water. The product was recrystallized by ethanol to obtain as pale yellow solid. The uniformity of the final products was monitored by ascending thin layer chromatography (TLC) on silica gel-G. All the solvents used were analytical reagent grade. FT-IR spectra of the products were recorded on a Shimadzu-FT-IR spectrometer (range 4000–400 cm<sup>-1</sup>) in KBr pellets. The UV Visible absorption spectra under investigation were recorded on Shimadzu-1650 in spectral grade methanol ( $\lambda_{max}$  in cm<sup>-1</sup>). <sup>1</sup>H NMR and <sup>13</sup>C NMR spectra for analytical purpose were recorded in CDCl<sub>3</sub> on a Bruker instrument at 400 MHz.

The products characterizations are shown below:

(*E*)-*N*-benzylidene-4-methylbenzo[d]thiazol-2-amine (3a): C<sub>15</sub>H<sub>12</sub>N<sub>2</sub>S; M.pt: 161–162 °C; UV Vis: 345, 222; FTIR (KBr, u/cm<sup>-1</sup>): (Ar–CH) 3024, (Ali–CH) 2922, (C=N<sub>thiazole</sub>) 1562, (CH=N) 1602, (C–S–C) 754; <sup>1</sup>H (NMR) (400 MHz, CDCl<sub>3</sub>, TMS):  $\delta$  7.07–8.19 (8H, m, Ar–H), 2.60 (3H, s, CH<sub>3</sub>), 8.11 (1H, s, N=CH); <sup>13</sup>C NMR (400 MHz, CDCl<sub>3</sub>):  $\delta$  18.1 (CH<sub>3</sub>), 169.4 (C=N<sub>thiazole</sub>), 146.1 (C=N), 145.6–118.9 (aromatic carbons).

(*E*)-*N*-(4-chlorobenzylidene)-4-methylbenzo[d]thiazol-2-amine (3b): C<sub>15</sub>H<sub>11</sub>N<sub>2</sub>SCl. M.pt: 130–131 °C; UV Vis: 323, 271; FTIR (KBr, u/cm<sup>-1</sup>): (Ar–CH) 3065, (Ali–CH) 2922, (C=N<sub>thiazole</sub>) 1551, (CH=N) 1613, (C–S–C) 745; <sup>1</sup>H NMR (400 MHz, CDCl<sub>3</sub>, TMS):  $\delta$  7.06–7.65 (8H, m, Ar–H), 2.59 (3H, s, CH<sub>3</sub>), 7.88 (1H, s, N=CH); <sup>13</sup>C NMR (400 MHz,



**Scheme 1** Synthesis of aryl imines over WO<sub>3</sub>/AITUD-1 catalyst

$\text{CDCl}_3$ ):  $\delta$  18.03 ( $\text{CH}_3$ ), 167.4 ( $\text{C}=\text{N}_{\text{thiazole}}$ ), 150.6 ( $\text{C}=\text{N}$ ), 142.8–118.7 (aromatic carbons).

(*E*)-4-methyl-*N*-(4-methylbenzylidene)benzo[*d*]thiazol-2-amine (3c):  $\text{C}_{16}\text{H}_{14}\text{N}_2\text{S}$ . M.pt.: 107–108 °C; UV Vis: 340, 225; FTIR (KBr,  $\text{u}/\text{cm}^{-1}$ ): (Ar–CH) 3064, (Al–CH) 2922, ( $\text{C}=\text{N}_{\text{thiazole}}$ ) 1551, ( $\text{CH}=\text{N}$ ) 1612, (C–S–C) 744;  $^1\text{H}$  NMR (400 MHz,  $\text{CDCl}_3$ , TMS):  $\delta$  7.06–7.65 (8H, m, Ar–H), 2.55 (3H, s,  $\text{CH}_3$ ), 2.39 (3H, s,  $\text{CH}_3$ ), 7.87 (1H, s,  $\text{N}=\text{CH}$ );  $^{13}\text{C}$  NMR (400 MHz,  $\text{CDCl}_3$ ):  $\delta$  18.1 ( $\text{CH}_3$ ), 167.4 ( $\text{C}=\text{N}_{\text{thiazole}}$ ), 150.6 ( $\text{C}=\text{N}$ ), 142.8–118.7 (aromatic carbons).

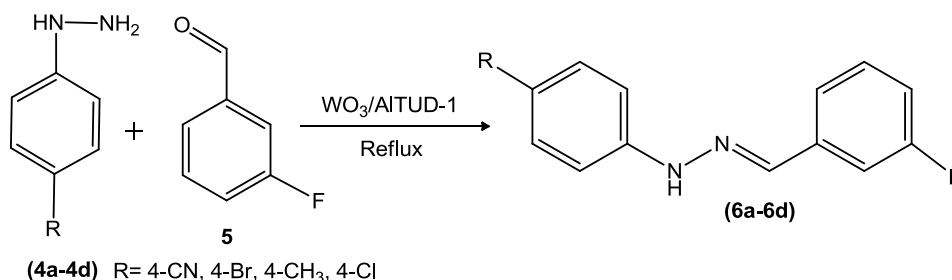
(*E*)-*N*-(4-methoxybenzylidene)-4-methylbenzo[*d*]thiazol-2-amine (3d):  $\text{C}_{16}\text{H}_{14}\text{N}_2\text{OS}$ . M.pt.: 149–150 °C; UV Vis: 338, 227; FTIR (KBr,  $\text{u}/\text{cm}^{-1}$ ): (Ar–CH) 3061, (Al–CH) 2924, ( $\text{C}=\text{N}_{\text{thiazole}}$ ) 1508, ( $\text{CH}=\text{N}$ ) 1601, (C–S–C) 741;  $^1\text{H}$  NMR (400 MHz,  $\text{CDCl}_3$ , TMS):  $\delta$  6.92–7.63 (8H, m, Ar–H), 2.54 (3H, s,  $\text{CH}_3$ ), 3.85 (3H, s,  $\text{OCH}_3$ ), 7.83 (1H, s,  $\text{N}=\text{CH}$ );  $^{13}\text{C}$  NMR (400 MHz,  $\text{CDCl}_3$ ):  $\delta$  18.1 ( $\text{CH}_3$ ), 55.4 ( $\text{OCH}_3$ ), 168.1 ( $\text{C}=\text{N}_{\text{thiazole}}$ ), 161.0 ( $\text{C}=\text{N}$ ), 148.6–114.2 (aromatic carbons).

(*E*)-4-methyl-*N*-(3-nitrobenzylidene)benzo[*d*]thiazol-2-amine (3e):  $\text{C}_{15}\text{H}_{11}\text{N}_3\text{O}_2\text{S}$ . M.pt.: 189–190 °C; UV Vis: 340, 226; FTIR (KBr,  $\text{u}/\text{cm}^{-1}$ ): (Ar–CH) 3088, (Al–CH) 2976, ( $\text{C}=\text{N}_{\text{thiazole}}$ ) 1533, ( $\text{CH}=\text{N}$ ) 1599, (C–S–C) 723;  $^1\text{H}$  NMR (400 MHz,  $\text{CDCl}_3$ , TMS):  $\delta$  7.07–8.22 (8H, m, Ar–H), 2.52 (3H, s,  $\text{CH}_3$ ), 8.48 (1H, s,  $\text{N}=\text{CH}$ );  $^{13}\text{C}$  NMR (400 MHz,  $\text{CDCl}_3$ ):  $\delta$  17.9 ( $\text{CH}_3$ ), 167.4 ( $\text{C}=\text{N}_{\text{thiazole}}$ ), 148.7 ( $\text{C}=\text{N}$ ), 141.9–119.1 (aromatic carbons).

## 2.4 Synthesis of hydrazones over $\text{WO}_3/\text{AITUD-1}$

In a typical reaction, equimolar quantities of 3-fluorobenzaldehyde (0.01 mol), substituted phenylhydrazine (0.01 mol) and 20 mL of ethanol with 0.1 g of  $\text{WO}_3/\text{AITUD-1}$  catalyst were added to 50 mL round bottom (RB) flask fitted with magnetic stirrer (Scheme 2). This solution was refluxed for 4 h and the reaction progress is monitored by TLC. After completion, the reaction mixture was cooled and washed with water. The product was recrystallized by ethanol to obtain as glittering solids. The uniformity of the final products was monitored by ascending TLC on silica gel-G.

**Scheme 2** Synthesis of phenylhydrazones over  $\text{WO}_3/\text{AITUD-1}$  catalyst



The obtained products characterizations are shown below:

(*E*)-4-(2-(3-fluorobenzylidene)hydrazinyl) benzonitrile (6a):  $\text{C}_{14}\text{H}_{10}\text{FN}_3$ ; Mol.Wt. 239; M.pt.: 190–191 °C; UV Vis: 346, 288; FTIR (KBr,  $\text{u}/\text{cm}^{-1}$ ): 3045 (Ar–CH), 3263 (Ar–NH), 1595 ( $\text{CH}=\text{N}$ );  $^1\text{H}$  NMR (400 MHz,  $\text{CDCl}_3$ ,  $\delta$ , ppm): 7.24–7.92 (m, 8H, Ar–H), 7.82 (s, 1H, NH) 7.98 (s, 1H,  $-\text{N}=\text{CH}-$ );  $^{13}\text{C}$  NMR (100 MHz,  $\text{CDCl}_3$ ,  $\delta$ , ppm): 148.3 ( $\text{CH}=\text{N}$ ), 144.5–106.3 (aromatic carbons).

(*E*)-1-(4-bromophenyl)-2-(3-fluorobenzylidene) hydrazine (6b):  $\text{C}_{13}\text{H}_{10}\text{BrFN}_2$ ; Mol.Wt. 292; M.pt.: 100–101 °C; UV Vis: 338, 248; FTIR (KBr,  $\text{u}/\text{cm}^{-1}$ ): 3078 (Ar–CH), 3255 (Ar–NH), 1647 ( $\text{CH}=\text{N}$ );  $^1\text{H}$  NMR (400 MHz,  $\text{CDCl}_3$ ,  $\delta$ , ppm): 7.14–7.85 (m, 8H, Ar–H), 7.86 (s, 1H, NH) 8.03 (s, 1H,  $-\text{N}=\text{CH}-$ );  $^{13}\text{C}$  NMR (100 MHz,  $\text{CDCl}_3$ ,  $\delta$ , ppm): 143.2 ( $\text{CH}=\text{N}$ ), 137.1–112.1 (aromatic carbons).

(*E*)-1-(3-fluorobenzylidene)-2-(4-tolyl) hydrazine (6c):  $\text{C}_{14}\text{H}_{13}\text{FN}_2$ ; Mol.Wt. 228; M.pt.: 122–123 °C; UV Vis: 338, 248; FTIR (KBr,  $\text{u}/\text{cm}^{-1}$ ): 3055 (Ar–CH), 3294 (Ar–NH), 1618 ( $\text{CH}=\text{N}$ );  $^1\text{H}$  NMR (400 MHz,  $\text{CDCl}_3$ ,  $\delta$ , ppm): 7.57–7.10 (m, 8H, Ar–H), 7.74 (s, 1H, NH) 7.91 (s, 1H,  $-\text{N}=\text{CH}-$ ); 2.28 (s, 3H,  $-\text{CH}_3$ );  $^{13}\text{C}$  NMR (100 MHz,  $\text{CDCl}_3$ ,  $\delta$ , ppm): 147.9 ( $\text{CH}=\text{N}$ ), 140.5–101.7 (aromatic carbons), 28.7 ( $\text{CH}_3$ ).

(*E*)-1-(4-chlorophenyl)-2-(3-fluorobenzylidene) hydrazine (6d):  $\text{C}_{13}\text{H}_{10}\text{ClFN}_2$ ; Mol.Wt. 248; M.pt.: 112–113 °C; UV Vis: 351, 310; FTIR (KBr,  $\text{u}/\text{cm}^{-1}$ ): 3053 (Ar–CH), 3315 (Ar–NH), 1591 ( $\text{CH}=\text{N}$ );  $^1\text{H}$  NMR (400 MHz,  $\text{CDCl}_3$ ,  $\delta$ , ppm): 7.00–7.90 (m, 8H, Ar–H), 7.62 (s, 1H, NH) 7.92 (s, 1H,  $-\text{N}=\text{CH}-$ );  $^{13}\text{C}$  NMR (100 MHz,  $\text{CDCl}_3$ ,  $\delta$ , ppm): 142.3 ( $\text{CH}=\text{N}$ ), 141.4–114.3 (aromatic carbons).

## 3 Results and discussion

### 3.1 Catalyst characterization

The high angle ( $2\theta = 5^\circ\text{--}80^\circ$ ) XRD patterns of AITUD-1 and typical  $\text{WO}_3/\text{AITUD-1}$  catalysts are depicted in Fig. 1. AITUD-1 and  $\text{WO}_3/\text{AITUD-1}$  exhibits a broad diffraction peak in the  $2\theta$  range of  $10^\circ\text{--}30^\circ$ , due to the presence of

amorphous silica ( $\text{SiO}_2$ ). An absence of alumina peaks in XRD patterns of AITUD-1, confirmed the complete incorporation of  $\text{Al}^{3+}$  into TUD-1 framework [28, 29]. Besides, the XRD patterns of the  $\text{WO}_3$ /AITUD-1 catalyst displayed the minimal diffraction peaks at  $23.6^\circ$ ,  $33.6^\circ$  and  $54.5^\circ$  related to  $\text{WO}_3$  crystalline species [23, 26]. This clearly indicated that the  $\text{WO}_3$  species are finely dispersed on internal porous walls and an external surface of TUD-1.

The  $\text{N}_2$  adsorption-desorption isotherms and pore size distribution of typical  $\text{WO}_3$ /TUD-1 catalyst are represented in Fig. 2. According to the IUPAC classification, type IV isotherm with H2 hysteresis loop is exhibited, indicating the characteristic of TUD-1 type wormhole pore architectures [23, 26, 29]. The steep desorption and sloping adsorption clearly indicate that the presence of interconnected porous networks [26]. Moreover, the isotherm showed a sharp variation at a relative pressure between 0.6 and 0.9 representing the typical capillary condensation within pores. It is found that catalyst exhibited a surface area of  $510 \text{ m}^2 \text{ g}^{-1}$ . The pore size distribution (Fig. 2b) measured from the desorption branch using the BJH model with a peak of around 6.4 nm. Also, the pore size distribution of the catalyst had narrow pore size distribution and the sharpness indicated the uniformity of mesopore distribution.

The FT-IR spectra of  $\text{WO}_3$ /AITUD-1 and AITUD-1 catalyst are shown in Fig. 3. The catalysts exhibited the bands at  $3450$ ,  $1640$ ,  $1223$ ,  $1100$  and  $803 \text{ cm}^{-1}$ . The bands at  $3450 \text{ cm}^{-1}$  and  $1640 \text{ cm}^{-1}$  are mainly caused by the O-H stretching vibration and bending vibration mode of the adsorbed water molecules or surface silanol groups (Si-O-H). Further, the peaks observed at  $1223$ ,  $1100$  and  $803 \text{ cm}^{-1}$  are due (Si-O-Si) asymmetric and symmetric stretching vibrations. The similar type of vibration bands were reported for metal (Co, Sn, Ti, Zr) containing TUD-1

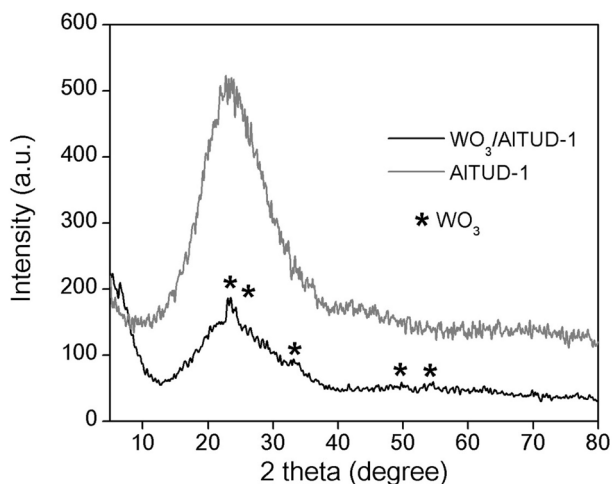


Fig. 1 Wide angle XRD of AITUD-1 and  $\text{WO}_3$ /AITUD-1

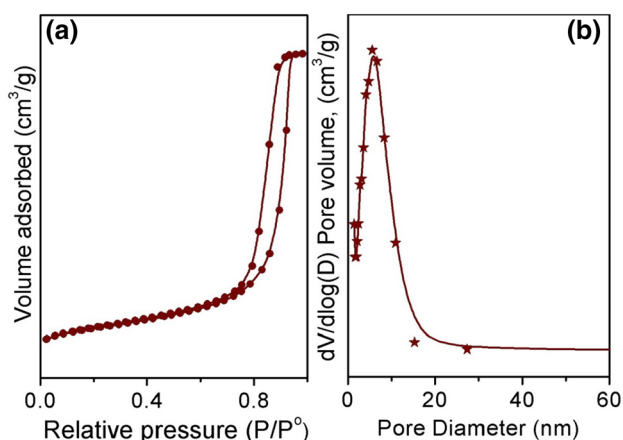


Fig. 2 **a**  $\text{N}_2$  adsorption-desorption isotherms and **b** BJH pore size distribution of  $\text{WO}_3$ /AITUD-1

silicates [29–32]. Noticeably, the vibration bands corresponding for  $\text{WO}_3$  in the  $\text{WO}_3$ /AITUD-1 catalyst are shielded by the bands of AITUD-1.

The FT-Raman spectra of  $\text{WO}_3$ /AITUD-1, AITUD-1, and  $\text{WO}_3$  are presented in Fig. 4. In comparison with  $\text{WO}_3$ /AITUD-1 and bulk  $\text{WO}_3$  four peaks were noticed at  $807$ ,  $718$ ,  $326$  and  $273 \text{ cm}^{-1}$  which confirms the presence of crystalline  $\text{WO}_3$  species [23]. These peaks are assigned to the deformation mode of W-O-W, symmetric stretching mode of W-O and bending mode of W-O, respectively [26, 27]. Apart from  $\text{WO}_3$  peaks, an intense band at  $976 \text{ cm}^{-1}$  was observed, which can be assigned to poly tungstate species or terminal bond W=O of the tetrahedrally coordinated  $\text{WO}_3$  over the AITUD-1 surface [27, 33]. Bhuiyan et al. [34] had assigned  $970 \text{ cm}^{-1}$  peak as the terminal W=O (symmetric stretching) mode of tungsten oxide

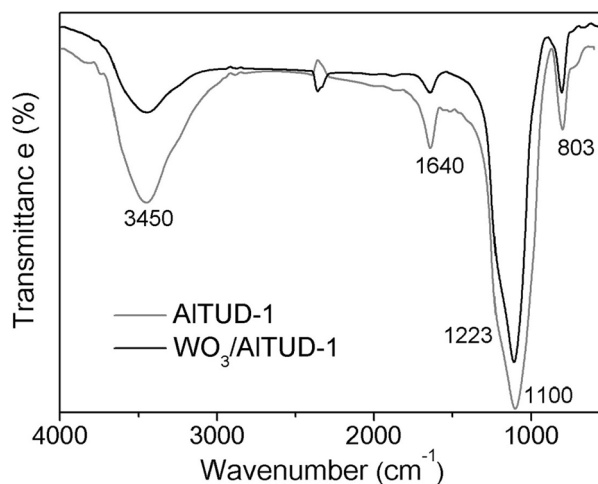
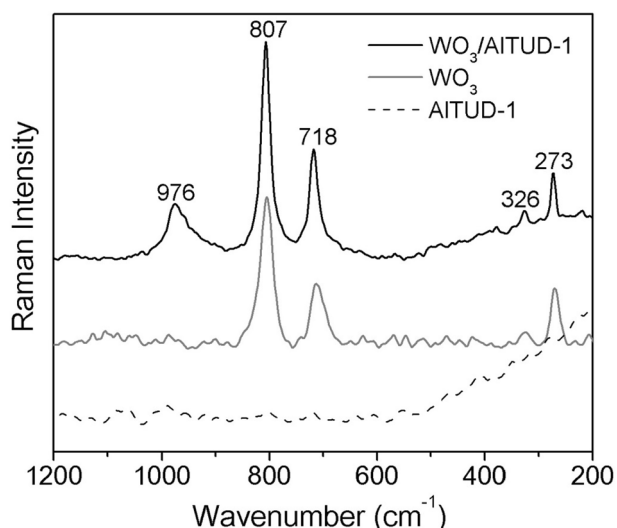


Fig. 3 FTIR spectra of AITUD-1 and  $\text{WO}_3$ /AITUD-1 sample



**Fig. 4** FT-Raman spectra AITUD-1, WO<sub>3</sub>/AITUD-1 and bulk WO<sub>3</sub>

(tetrahedrally coordinated) species, which are active sites for metathesis reactions.

SEM and TEM micrographs of WO<sub>3</sub>/AITUD-1 are shown in Fig. 5. From the SEM image (Fig. 5a), the sample showed the disordered shapes with micrometer size of SiO<sub>2</sub> particles with dispersed WO<sub>3</sub> particles. The sponge- or wormhole-like three-dimensionally connected mesopore network which is typical for TUD-1 materials was further confirmed by TEM [31, 32] (Fig. 5b). Furthermore, due to low WO<sub>3</sub> loading and contrast, it was difficult to identify the metal oxide phases in TEM image. The presence of Al, W and Si are confirmed by the ICP-OES and its quantities are similar to synthesis composition.

The UV-vis diffuse reflectance absorption spectrum of WO<sub>3</sub>/AITUD-1 is displayed in Fig. 6. A broad peak around 200–450 nm in the catalyst is due to the overlapping bands of isolated tetrahedral [WO<sub>4</sub>]<sup>2-</sup> species (240 nm), low oligomeric tungsten oxide species (290 nm) and crystalline WO<sub>3</sub> (380 and 450 nm) [21, 26, 27]. However, the absorbance

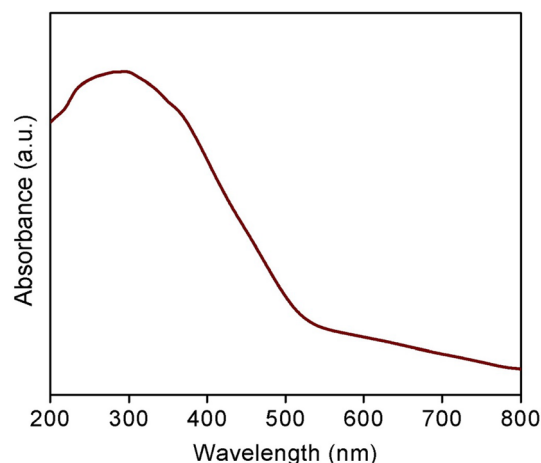


**Fig. 6** DR UV Vis of WO<sub>3</sub>/AITUD-1

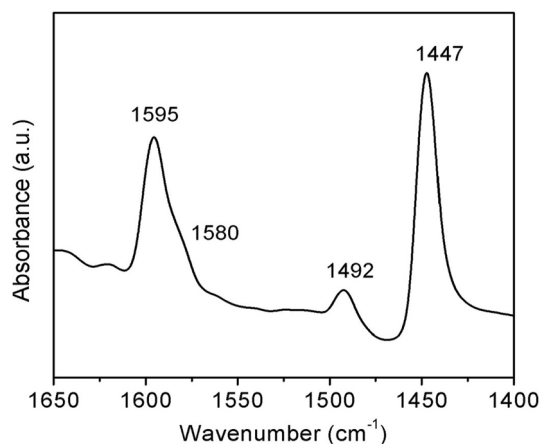
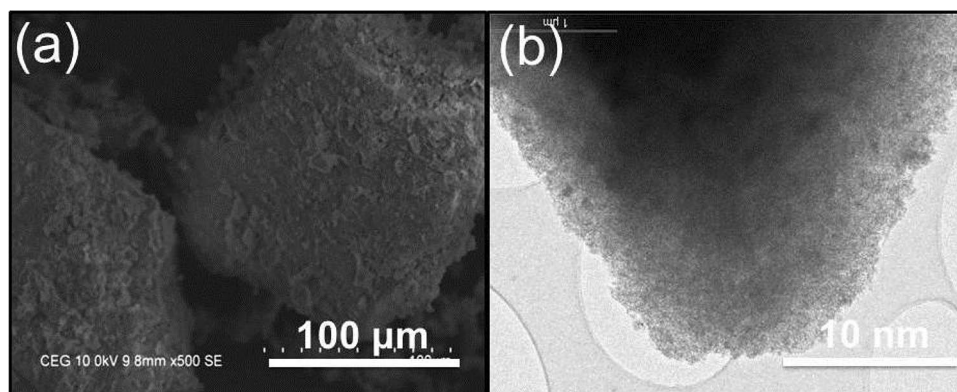


**Fig. 7** FT-IR spectrum of pyridine adsorbed WO<sub>3</sub>/AITUD-1

peak values are varied based on the W species (incorporated W or WO<sub>x</sub>) and the architecture of mesoporous materials. The FT-IR spectrum of pyridine adsorbed on WO<sub>3</sub>/AITUD-1 catalyst in the region of 1650–1400 cm<sup>-1</sup> is

**Fig. 5** **a** SEM and **b** TEM images of WO<sub>3</sub>/AITUD-1



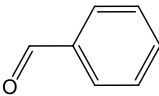
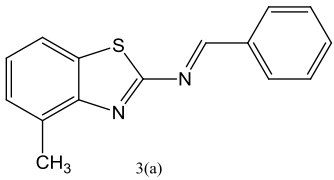
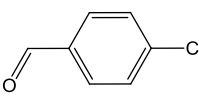
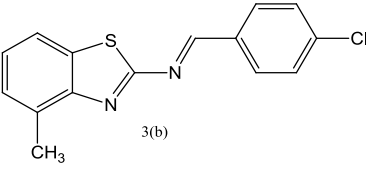
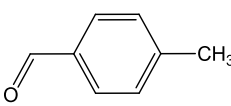
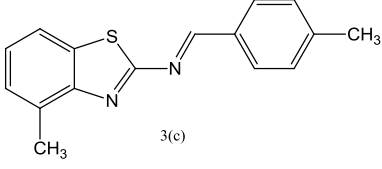
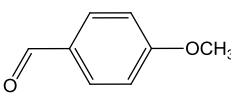
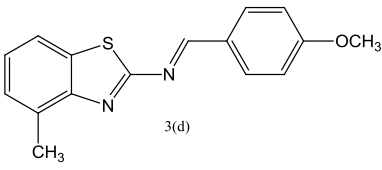
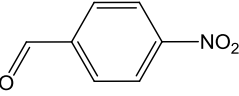
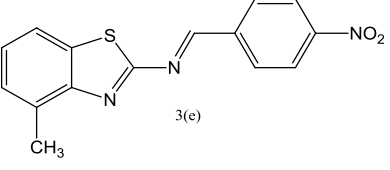
depicted in Fig. 7. The bands at 1595 and 1447  $\text{cm}^{-1}$  are due to the pyridine bonded to the Lewis acid sites [30, 32]. On the other hand, the band at 1492  $\text{cm}^{-1}$  is due to the combinations of Lewis and Bronsted acid sites [26]. Besides, AITUD-1 leads to an increase in the Lewis acidity.

### 3.2 Catalyst reactions

The reaction conditions such as time, solvent, catalyst amount and temperature were optimized by screening as given in Schemes 1 and 2. Maximum yield was obtained at 80 °C temperature, 20 mL of the solvent (ethanol), 0.1 g of catalyst and 4 h refluxing time. Further, we extended these

optimized reaction conditions to differently substituted benzaldehydes with 4-methyl substituted benzo[*d*]thiazol-2-amine and the obtained results are presented (Table 1). Notably, 83% of the maximum yield was obtained using the  $\text{WO}_3$ /AITUD-1 as a catalyst. Substituted benzaldehyde with groups  $-\text{Cl}$ ,  $-\text{NO}_2$ ,  $-\text{OCH}_3$  and  $-\text{CH}_3$  (electron donating and withdrawing) groups in *para* position produce the corresponding products in good yields (70–80%). Similarly, 3-fluoro aldehyde reacts with different electron withdrawing and electron donating substituted hydrazine produces good yields (75–80%) as shown in Table 2. The yield of products clearly indicates the good dispersion of active  $\text{WO}_3$  and incorporated  $\text{Al}^{3+}$  species on the large porous

**Table 1** Synthesis of different group substituted (*E*-*N*-benzylidene-4-methylbenzo[*d*]thiazol-2-amine) compounds

No.	Aromatic aldehydes (X)	Product	Yield <sup>a</sup> (%)
1			83
2			80
3			74
4			76
5			82

Reaction conditions: Aromatic aldehydes (0.01 mol), 4-methylbenzo[*d*]thiazol-2-amine (0.01 mol), ethanol (20 mL), temperature (80 °C), catalyst (0.1 g) time (4 h)

<sup>a</sup>Isolated yield

**Table 2** Synthesis of different phenylhydrazone compounds

No.	Aromatic hydrazines (X)	Product	Yield <sup>a</sup> (%)
1			82
2			80
3			78
4			81

Reaction conditions: aldehyde (0.01 mol), substituted hydrazines (0.01 mol), ethanol (20 mL), temperature (80 °C), catalyst (0.1 g) time (4 h)

<sup>a</sup>Isolated yield

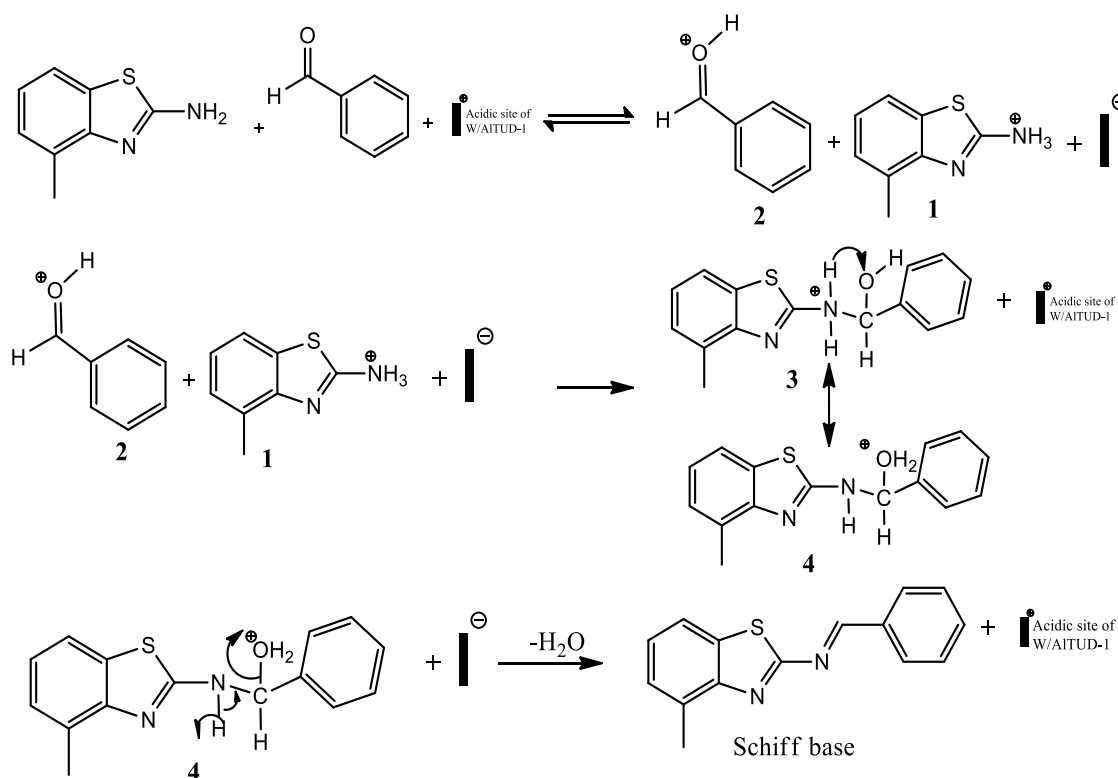
TUD-1 support materials and interactions taking place between  $WO_3$  species and the AITUD-1 support [27].

The generally accepted mechanism of Schiff base reaction was proposed by many researchers [35, 36]. By following the mechanism reported by Kumar et al. [37] acid catalysed reaction mechanism is proposed in Scheme 3. The mechanism involves the protonation of both Schiff base and aldehyde with acidic  $WO_3$ /AITUD-1 catalyst to option intermediate (1) and (2). This protonated Schiff base intermediate (1) attacked the carbonyl carbon of the intermediate (2) which gives intermediate (3) followed by proton transfer from nitrogen to oxygen to give an intermediate (4). This on further dehydration and deprotonation to produces imines. The solid acid catalyst ( $WO_3$ /AITUD-1) promotes dehydration and deprotonation.

## 4 Conclusions

In summary, finely dispersed tungsten oxide ( $WO_3$ ) introduced mesoporous AITUD-1 support was successfully synthesized by a modest synthesis procedure. The characterization studies confirmed amorphous, mesoporous and wormhole nature of the catalyst. This  $WO_3$ /AITUD-1 catalyst was presented as an efficient catalyst for synthesis of 1-substituted benzylidene-4-methylbenzo[d]thiazole-2-amines (thiazo aryl imines) and phenylhydrazones ~70–80% of the yield in the optimum reaction conditions. The solid acid catalyst ( $WO_3$ /AITUD-1) promotes dehydration and deprotonation owing to the presence of acidic sites (B+L). The catalytic activity related to framework incorporated  $Al^{3+}$ , dispersed  $WO_3$  and the good





**Scheme 3** The proposed mechanism for the formation Schiff base over  $\text{WO}_3/\text{AITUD-1}$  catalyst

accessibility of these active sites to the reactants. Hence, we developed an efficient and simple alternative for the preparation of substituted benzo[d]thiazol-2-amines and phenylhydrazones via three-dimensional mesoporous acid catalyst under feasible reaction method. Further the studies will extend against other microbial species. Also, this catalyst can be exploited for the study of other heterogeneous acid catalysed organic transformations.

## 5 Supplementary information (SI)

The UV visible, FTIR and NMR ( $^1\text{H}$  and  $^{13}\text{C}$ ) spectral data of selective compounds are available in supplementary information (Figures S1–S12).

**Acknowledgments** The authors extend their appreciation to the Deanship of Scientific Research at King Khalid University for funding this work through General Research Project under Grant Number (R.G.P.1/45/39). The author MR thankful to the Department of Physics, Annamalai University, Annamalainagar-608002 for recording UV and IR spectral analysis. The author MPP thanks the Department of Chemistry, Anna University Chennai for the characterization supports.

## Compliance with ethical standards

**Conflict of interest** The authors declare that they have no conflict of interest.

## References

- Lau KY, Mayr A, Cheung KK (1999) Synthesis of transition metal isocyanide complexes containing hydrogen bonding sites in peripheral locations. *Inorg Chim Acta* 285(2):223
- Shawali AS, Harb NMS, Badahdah KO (1985) A study of tautomerism in diazonium coupling products of 4-hydroxycoumarin. *J Heterocycl Chem* 22(5):1397
- Kajal A, Bala S, Kamboj S, Sharma N, Saini V (2013) Schiff bases: a versatile pharmacophore. *J Catal* 2013:1
- Vicini P, Geronikaki A, Incerti M, Busonera B, Poni G, Cabrasca CA, Colla PL (2003) Synthesis and biological evaluation of benzo[d]isothiazole, benzothiazole and thiazole Schiff bases. *Bioorg Med Chem* 11:4785
- Grossmann K, Caspar G, Kwiatkowski J, Bowe SJ (2002) On the mechanism of selectivity of the corn herbicide BAS 662H: a combination of the novel auxin transport inhibitor diflufenzopyr and the auxin herbicide dicamba. *Pest Manag Sci* 58:1002–1014
- Dimmock JR, Vashishtha SC, Stables JP (2000) Anticonvulsant properties of various acetylhydrazones, oxamoylhydrazones and semicarbazones derived from aromatic and unsaturated carbonyl compounds. *Eur J Med Chem* 35:241–248

- Rajarajan M, Senbagam R, Vijayakumar R, Manikandan V, Balaji S, Vanangamudi G, Thirunarayanan G (2016) Synthesis, spectral correlations and antimicrobial activities of substituted 4-((E)-2-benzylidenehydrazinyl)benzotrile compounds. *Indian J Chem* 55B:197
- Kaugars G, Gemrich EG, Rizzo VL (1973) Miticidal activity of benzoyl chloride phenylhydrazones. *J Agric Food Chem* 21:647–650
- Belkheiri N, Bouguerne B, Bedos-Belval F, Duran H, Bemis C, Salvayre R, Negre-Salvayre A, Baltas M (2010) Synthesis and antioxidant activity evaluation of a syringic hydrazones family. *Eur J Med Chem* 45:3019–3026
- Wiley RH, Clevenger RL (1962) Aldehyde hydrazone derivatives in cancer chemotherapy. *J Med Pharm Chem* 5:1367–1371
- Rajarajan M, Senbagam R, Vijayakumar R, Manikandan V, Balaji S, Vanangamudi G, Thirunarayanan G (2016) Eco-friendly synthesis, spectral correlation analysis, and antimicrobial activities of substituted (E)-1-benzylidene-2-(3-nitrophenyl)hydrazines. *Orbital: Electron J Chem* 8(5):288–299
- Ravi K, Krishnakumar B, Swaminathan M (2012) An efficient protocol for the green and solvent-free synthesis of azine derivatives at room temperature using  $\text{BiCl}_3$ -loaded montmorillonite K10 as a new recyclable heterogeneous catalyst. *ISRN Org Chem* 2012:1
- Branchaud BP (1983) Studies on the preparation and reactions of tritylsulfenimines. *J Org Chem* 48:3531
- Bazgir A (2006) Microwave-assisted efficient synthesis of diimines in dry media using silica gel supported sodium hydrogen sulfate as reusable solid support. *J Chem Res* 37:1
- Polshettiwar V, Varma RS (2008) Greener and expeditious synthesis of bioactive heterocycles using microwave irradiation. *Pure Appl Chem* 80(4):777
- Abid M, Savolainen M, Landge S, Hu J, Suryaprakash GK, Olah GA, Torok B (2007) Synthesis of trifluoromethyl-imines by solid acid/superacid catalyzed microwave assisted approach. *J Fluor Chem* 128:587
- Barr DA, Donegn G, Grigg R (1989) Tandem Michael addition–1,3-dipolar cycloaddition of imines of  $\alpha$ -amino acid esters and aminoacetonitrile. *J Chem Soc Perkin Trans* 1:1550
- Chakraborti AK, Bhagat S, Rudrawar S (2004) Magnesium perchlorate as an efficient catalyst for the synthesis of imines and phenylhydrazones. *Tetrahedron Lett* 45:7641
- Dutheuil G, Bonnaire SC, Pannecoucke X (2007) Diastereomeric fluoroolefins as peptide bond mimics prepared by asymmetric reductive amination of  $\alpha$ -fluoroenones. *Angew Chem Int Ed Engl* 46:1312
- Devidas SM, Quadri SH, Kamble SA, Syed FM, Vyavhare DY (2011) Novel one-pot synthesis of schiff base compounds derived from different diamine & aromatic aldehyde catalyzed by  $\text{P}_2\text{O}_5/\text{SiO}_2$  under free-solvent condition at room temperature. *J Chem Pharm Res* 3(2):489
- Maheswari R, Pachamuthu MP, Ramanathan A, Subramaniam B (2014) Synthesis, characterization, and epoxidation activity of tungsten-incorporated SBA-16 (W-SBA-16). *Ind Eng Chem Res* 53:18833
- Yan W, Ramanathan A, Ghanta M, Subramaniam B (2014) Towards highly selective ethylene epoxidation catalysts using hydrogen peroxide and tungsten or niobium-incorporated mesoporous silicate (KIT-6). *Catal Sci Technol* 4:4433
- Zhang YQ, Wang SJ, Wang JW, Lou LL, Zhang C, Liu S (2009) Synthesis and characterization of Zr-SBA-15 supported tungsten oxide as a new mesoporous solid acid. *Solid State Sci* 11:1412
- Bordoloi A, Halligudi SB (2010) Catalytic properties of  $\text{WO}_x/\text{SBA-15}$  for vapor-phase Beckmann rearrangement of cyclohexanone oxime. *Appl Catal Gen* 379A:141
- Kundu SK, Mondal J, Bhaumik A (2013) Tungstic acid functionalized mesoporous SBA-15: a novel heterogeneous catalyst for facile one-pot synthesis of 2-amino-4H-chromenes in aqueous medium. *Dalton Trans* 42:10515
- Ten Dam J, Badloe D, Ramanathan A, Djanashvili K, Kapteijn F, Hanefeld U (2013) Synthesis, characterisation and catalytic performance of a mesoporous tungsten silicate: W-TUD-1. *Appl Catal Gen* 468:150
- Pachamuthu MP, Maheswari R, Ramanathan A (2017) Synthesis and characterizations of isolated  $\text{WO}_4$  anchored on Mesoporous TITUD-1 support. *Appl Surf Sci* 402:286
- Anand R, Maheswari R, Hanefeld U (2006) Catalytic properties of the novel mesoporous aluminosilicate AITUD-1. *J Catal* 242:82
- Pasupathi M, Santhi N, Pachamuthu MP, Alamelu Mangai G, Ragupathi C (2018) Aluminium and titanium modified mesoporous TUD-1: a bimetal acid catalyst for biginelli reaction. *J Mol Struct* 1160:161
- Pachamuthu MP, Shanthi K, Luque R, Ramanathan A (2013) SnTUD-1: a solid acid catalyst for three component coupling reactions at room temperature. *Green Chem* 15:2158
- Pachamuthu MP, Rajalakshmi R, Maheswari R, Anand R (2014) Direct glycol assisted synthesis of amorphous mesoporous silicate with framework incorporated  $\text{CO}^{2+}$  characterization and catalytic application in ethylbenzene oxidation. *RSC Adv* 4:29909
- Pachamuthu MP, Srinivasan VV, Maheswari R, Shanthi K, Ramanathan A (2013) Lewis acidic ZrTUD-1 as catalyst for tert-butylation of phenol. *Appl Catal Gen* 462:143
- Mishra G, Behera GC, Singh SK, Parida KM (2012) Liquid phase esterification of acetic acid over  $\text{WO}_3$  promoted  $\beta$ -SiC in a solvent free system. *Dalton Trans* 41:14299
- Bhuiyan TI, Arudra P, Akhtar MN, Aitani AM, Abudawoud RH, Al-Yami MA, Al-Khattaf SS (2013) Metathesis of 2-butene to propylene over W-mesoporous molecular sieves: a comparative study between tungsten containing MCM-41 and SBA-15. *Appl Catal Gen* 467:224
- Suresh R, Kamalakkannan D, Ranganathan K, Arulkumaran R, Sundararajan R, Sakthnathan SP, Vijayakumar S, Sathiyamoorthi K, Mala V, Vanangamudi G, Thirumurthy K, Mayavel P, Thirunarayanan G (2013) Solvent-free synthesis, spectral correlations and antimicrobial activities of some aryl imines. *Spectrochim Acta* 101A:239–248
- Suresh R, Sakthnathan SP, Kamalakkannan D, Ranganathan K, Sathiyamoorthi K, Mala V, Arulkumaran R, Vijayakumar S, Sundararajan R, Vanangamudi G, Subramanian M, Thirunarayanan G, Vanaja G, Kanagambal P (2015) Solvent-free synthesis of azomethines, spectral correlations and antimicrobial activities of some E-benzylidene-4-chlorobenzenamines. *Bull Chem Soc Ethiop* 29(2):275–290
- Kumar A, Krishnakumar B, Sobral AGFN, Subash B, Swaminathan M, Sankaran KR (2016) An efficient, rapid and solvent-free synthesis of branched imines using sulphated anatase-titania as a novel solid acid catalyst. *Indian J Chem* 55B:1231–1238

**Publisher's Note** Springer Nature remains neutral with regard to jurisdictional claims in published maps and institutional affiliations.